

Evaluation of multi-RCM high-resolution hindcast over the CORDEX East Asia Phase II region: Mean, annual cycle and interannual variations

Ke Yu^{1,2} | Pinhong Hui³ | Weidan Zhou^{1,2} | Jianping Tang^{1,2} 

¹Key Laboratory of Mesoscale Severe Weather/Ministry of Education, Nanjing University, Nanjing, China

²School of Atmospheric Sciences, Nanjing University, Nanjing, China

³Jiangsu Climate Center, Jiangsu Provincial Meteorological Bureau, Nanjing, China

Correspondence

Jianping Tang, School of Atmospheric Sciences, Nanjing University, 163 Xianlin Road, Nanjing, China.

Email: jptang@nju.edu.cn

Funding information

National Key Research and Development Program of China, Grant/Award Numbers: 2016YFA0600303, 2018YFA0606003; National Natural Science Foundation of China, Grant/Award Number: 41875124

Abstract

Based on the Coordinated Regional Downscaling Experiment-East Asia second phase (CORDEX-EA-II) with higher resolution, model results driven by ERA-Interim reanalysis using WRF, RegCM4 and CCLM are evaluated against the observational datasets including CN05.1, CRU and GPCP during the period of 1989–2009. The results show that the RCMs have the capability to simulate the annual and seasonal mean surface air temperature and precipitation, however, some biases are produced. The biases are highly dependent on the geophysical locations and the RCMs applied, and CCLM agrees better with the observed precipitation over ocean. CCLM also outperforms the other two RCMs in simulating the interannual variations of temperature and precipitation in most sub-regions, which can be attributed to its better presentation of the interannual variation of large scale circulation. Generally, all the three RCMs can well reproduce the seasonal cycles of the surface air temperature in most sub-regions, however, only in the northern regions of China can the RCMs well reproduce the seasonal cycles of precipitation.

KEY WORDS

CORDEX, East Asia, regional climate model

1 | INTRODUCTION

Affected by the monsoon system, East Asia is expected to be one of the most vulnerable regions of global climate change (Jiang and Wang, 2005). Due to its unique geographical location and vegetation distribution, large variability is the main feature of the climate, including seasonal, interannual and decadal variations. Under the global warming background, the climate change of East Asia attracted broad attention among the government and the public. Many studies have investigated the climate change over East Asia using global climate models (GCMs) (Zhou and Zou, 2002; Mukai *et al.*, 2008; Lau and Poshay, 2009). However, GCMs have critical limitation in producing high-resolution regional climate information due to their relative coarse

resolution. And the complexity and diversity of physical processes should be detailedly represented in the climate models to better simulate climate change over East Asia. To generate more detailed spatial and temporal climate information, regional climate models (RCMs), as the dynamical downscaling tools, have been increasingly used to produce climate change information at the regional scale due to their higher resolution and better representation of the key physical processes (Tselioudis *et al.*, 2012; Cha *et al.*, 2016; Sun *et al.*, 2016; Yang *et al.*, 2017).

Since 1990s, RCMs have been widely applied over East Asia for regional climate simulation (Gao and Giorgi, 2017), future climate projection (Gao *et al.*, 2008), physical processes study (Yhang and Hong, 2006) and extreme climate events prediction (Park *et al.*, 2016). Using the Regional

Integrated Environment Modelling System, version 2.0 (RIEMS2.0), Zhao (2013) tested the ability of RIEMS2.0 to simulate long-term climate and climate changes in East Asia and to provide a basis for further development and applications. The role of horizontal resolution on the projection of future climate over China was investigated using a regional climate model RegCM4 (Shi *et al.*, 2017). Ji and Kang (2015) also simulated the changes of extreme climate events at the end of the 21st century with RegCM4, and found that the model simulated temperature extremes more accurately than precipitation. Although many regional climate simulations have been conducted over East Asia with RCMs, most of them use single RCM, which may induce systematic biases due to model dynamic and physical parameterization. To alleviate the uncertainties of the single RCM, the multi-RCM ensembles have been adopted in regional climate downscaling experiments through several international projects during the past decade (Fu *et al.*, 2005; Christensen *et al.*, 2007). Recently, an international downscaling project known as the Coordinated Regional Downscaling Experiment (CORDEX, <http://www.cordex.org/>), which aimed to produce an improved generation of regional climate change projections worldwide and provide a framework for better coordination of regional climate downscaling, was established by the World Climate Research Program (WCRP) (Giorgi *et al.*, 2009).

The CORDEX East Asia (CORDEX-EA) domain is one of the 14 target regions set by the CORDEX in its first plan (CORDEX-EA-I), which has the horizontal resolution at 0.44° (about 50 km). Many works have been done to investigate the regional variability and to project the future climate following the CORDEX-EA-I framework (Park *et al.*, 2013; Jin *et al.*, 2016; Zou *et al.*, 2016; Shen *et al.*, 2017; Tang *et al.*, 2017; Wang *et al.*, 2018). Park *et al.* (2013) investigated the impacts of boundary conditions on the precipitation simulation of RegCM4 in the CORDEX East Asia domain, and showed that RegCM4 adequately simulated the spatial distribution of precipitation and its temporal variations over the East Asia region, irrespective of the driving data used. Dosio *et al.* (2015) compared the results of the consortium for small-scale modelling (COSMO) regional climate model (COSMO-CLM; CCLM) to those of several driving GCMs, and found that the CCLM was generally able to improve the simulation of the annual cycle of precipitation, the probability distribution function of daily precipitation and the impact-relevant precipitation indices. Using a regional ocean–atmosphere coupled model and a stand-alone RCM, the effects of regional air-sea couplings on the simulations of East Asian summer monsoon rainfall have been investigated (Zhou *et al.*, 2016). Tang *et al.* (2017) studied the impact of the spectral nudging method on the regional climate simulation over the CORDEX-EA-I region using the Weather Research and Forecasting model (WRF). In general, these results of CORDEX-EA-I show that

RCM can basically reproduce the seasonal average and seasonal variation of the surface air temperature and precipitation in East Asia, but the individual model has larger differences and biases in individual regions and seasons. Currently, with the development of high performance computing, CORDEX-EA is advancing the second phase of higher resolution (CORDEX-EA-II), which comprises new regions and higher resolution (0.22°, about 25 km). One of the key issues in CORDEX-EA is multi-RCM ensemble. It is very important to evaluate the RCMs' performance before their application in the future climate projections.

Model evaluation is a fundamental step to assess the RCM's performance in reproducing the present climate, and to describe the error characteristics of RCM. It is essential to characterize its strength, weakness and uncertainty before the application in the future climate projection (Hong *et al.*, 2010; Kim *et al.*, 2014; Kotlarski *et al.*, 2014). The performance of RCM can be affected by many factors, including the model dynamics, physical processes and large-scale driving fields. One of the most common ways to assess RCM is to perform “perfect boundary condition experiments” (Christensen *et al.*, 1997). That is, regional climate models are driven by atmospheric reanalysis data, and then the model outputs are compared against reference data from observations to minimize systemic bias due to the large-scale global model itself (Rummukainen, 2010). Model evaluation can be further used to guide model development and/or for bias correction. Measuring model performance is important for applying multi-RCM ensemble.

This study aims to evaluate the capability of three RCMs within CORDEX-EA-II to simulate the mean climate, seasonal cycle and interannual variability as compared to observation. The evaluation is based on the “perfect” boundary condition experiments, which use reanalysis as large-scale forcing. Section 2 provides details of the experimental design, reference datasets and evaluation methods. Section 3 presents the evaluation of RCM skill in simulating the regional climate over CORDEX-EA-II. Results are summarized in Section 4.

2 | MODELS, DATA AND METHODOLOGY

2.1 | Models and experimental design

In this study, two nonhydrostatic RCMs (Weather Research and Forecasting model (WRF) and the COSMO model in Climate Mode (CCLM)) and one hydrostatic RCM (the Abdus Salam International Centre for Theoretical Physics (ICTP) Regional Climate Model version 4 (RegCM4)) are used to perform long-term regional climate simulations over East Asia. The WRFV3 (V3.6.1, Skamarock *et al.*, 2008), is

the most popular mesoscale model with a fully compressible, nonhydrostatic dynamic core and a terrain-following vertical coordinate. It has various physical schemes and dynamical options that can capture weather phenomena as well as climate features. The three-dimensional nonhydrostatic regional climate model CCLM is the climate version of the operational weather forecast model COSMO (Baldauf *et al.*, 2011) of the German Weather Service (GWS). It has a regular latitude/longitude grid (Arakawa-C grid) with a rotated pole and a terrain following height coordinate (Rockel *et al.*, 2008; Zhou *et al.*, 2016), and can describe the atmospheric circulation at resolutions between 1 and 50 km. The RegCM4, developed by the ICTP (Giorgi *et al.*, 2012), is a limited-area model based on a terrain-following σ -pressure vertical coordinate system and an Arakawa-B grid finite differencing algorithm. It has the hydrostatic dynamic component from the Pennsylvania State University Mesoscale Model version 5 (MM5; Grell *et al.*, 1994). All these RCMs have been widely used for regional climate modelling studies with seasonal to decadal time scales over East Asia (Ji and Kang, 2015; Jin *et al.*, 2016; Zhou *et al.*, 2016).

Following CORDEX-EA-II framework, the simulation domain (Figure 1) covers most of Asia, the western Pacific, the Bay of Bengal, and the South China Sea with the horizontal resolution at 25 km (WRF, RegCM4) or 0.22° (CCLM). Five sub-regions are chosen to detailedly evaluate the RCMs' simulation skills, which are South China (SC), Yangtze-Huaihe River Basin (YHR), North China (NC), Northeast China (NEC), Northwest China (NWC), India and Indo-China. All models employ the sponge lateral buffer zone with several grids at each direction, where the Davies boundary relaxation scheme is used (Davies, 1976) to remove possible impact of boundary bias. Different dynamic framework and physical schemes including convection, land

surface, planetary boundary layer (PBL), and radiations used in this study for these RCMs are summarized in Table 1. The physical schemes of these RCMs are similar to that used in the regional climate experiments over CORDEX-EA-I domain (Park *et al.*, 2013; Tang *et al.*, 2017). For all the three RCMs, the initial and lateral boundary conditions for the large-scale atmospheric fields are from the European Centre for Medium-Range Weather Forecasts (ECMWF) ERA-Interim reanalysis (ERA-Interim) (Dee *et al.*, 2011), which has a $0.75^\circ \times 0.75^\circ$ horizontal resolution. The sea surface temperatures (SSTs) are updated by using the Optimum Interpolation Sea Surface Temperature (OISST) weekly data from the National Ocean and Atmospheric Administration (Reynolds *et al.*, 2002). All the RCM experiments run continuously for 22 years from 1 January 1988 to 31 December 2009, and the first year (1988) is used as spin-up time. We conduct all the experiments without using the method of spectral nudging.

2.2 | Observation datasets

To assess the general ability of the regional climate models to reproduce the climate over the 21-year period (1989–2009), the simulated climate fields are compared with the ERA-Interim reanalysis and different surface observational datasets, including surface air temperature and precipitation. Over China, the observational dataset for the surface air temperature and precipitation are from the gridded daily scale dataset, CN05.1, which is developed by Wu and Gao (2013) from the National Climate Center (NCC) of China Meteorological Administration (CMA). The CN05.1 gridded dataset is based on interpolation from more than 2000 surface observations in China, and has a relative high spatial resolution of $0.25^\circ \times 0.25^\circ$ (latitude-longitude). For other

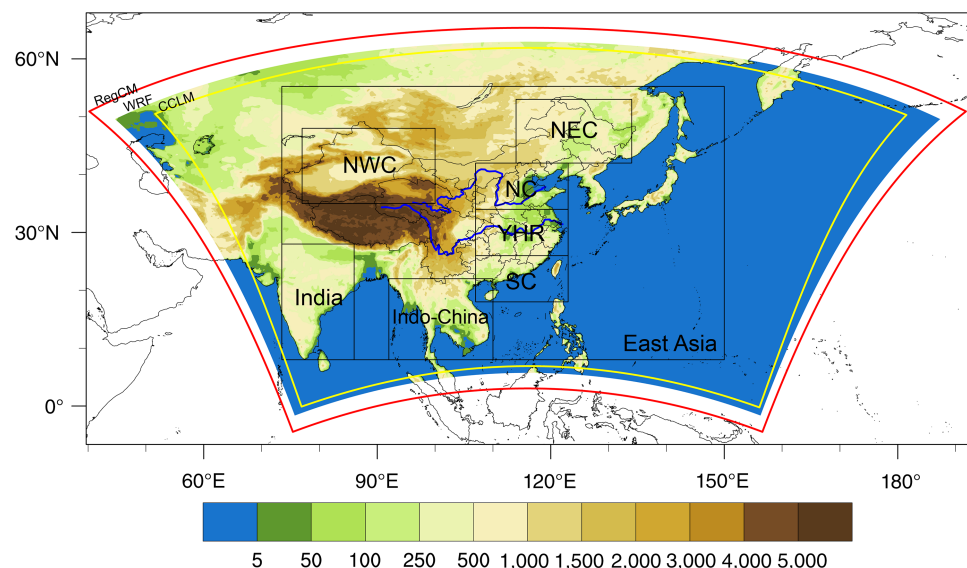


FIGURE 1 RCM simulation domain and the 7 sub-regions: East Asia, Northeast China (NEC), North China (NC), Yangtze-Huaihe River basin (YHR), South China (SC), Northwest China(NWC), India and Indo-China region

TABLE 1 Model configuration in this study

	WRF	RegCM	CCLM
Horizontal resolution(lat × lon)	25 km (252 × 384)	25 km (277 × 397)	0.22° (251 × 396)
Vertical levels	σ-30	σ-18	σ-40
Dynamic framework	Non-hydrostatic	Hydrostatic	Non-hydrostatic
Convection scheme	Kain-Fritsch (Kain 2004)	MIT (Emanuel and Živković-Rothman 1999)	Tiedtke (1989)
Land surface	Noah (Chen and Dudhia 2001)	BATS (Dickinson <i>et al.</i> 1993)	TERRA_ML (Schrodin and Heise 2001)
PBL scheme	YSU (Hong <i>et al.</i> 2006)	Modified Holtslag (Holtslag <i>et al.</i> 1990)	TKE level 2.5 (Mironov and Raschendorfer 2001)
Microphysics parameterization	WSM5 (Hong <i>et al.</i> 2004)	SUBEX (Pal <i>et al.</i> 2000)	Seifert and Beheng (2001)
Radiation	CAM (Collins <i>et al.</i> 2004)	Modified CCM3 (Kiehl <i>et al.</i> 1996)	Ritter and Geleyn (1992)
Subgrid terrain parameterization		Giorgi <i>et al.</i> (2003)	Lott and Miller (1997)
References	Skamarock <i>et al.</i> (2008)	Giorgi <i>et al.</i> (2012)	Doms and Baldauf (2015)
Initial and boundary conditions	ERA-interim reanalysis		
Simulation period	1989–2009		

regions in the CORDEX-EA-II domain, the monthly observational datasets are used, which are monthly surface air temperature from Climate Research Unit (CRU) (Harris *et al.*, 2014) and monthly precipitation from the Global Precipitation Climatology Project (GPCP v3.23) (Adler *et al.*, 2003). The CRU surface air temperature data is based on observations from over 4,000 meteorological stations worldwide provided by the WMO Observatory, and the observed data is interpolated to global land area with a resolution of 0.5°. The GPCP precipitation data is a global merged satellite and rain gauge dataset with a resolution of 2.5°. All these reference datasets have been widely used in climate model evaluation. For convenience, the reference datasets are merged together to cover the whole CORDEX-EA-II domain, and the CN05.1 dataset is used over China. The two merged datasets are CN05.1_CRU for temperature and CN05.1_GPCP for precipitation. And all the model simulated climate fields and merged reference datasets are interpolated to 0.25° × 0.25° grids. The interpolation method used by WRF and RegCM is simple inverse distance squared weighting, while CCLM applies first order conservative remapping, and the merged reference datasets are interpolated by bilinear interpolation method.

2.3 | Evaluation methods

To quantify the performance of RCMs, the common statistical measures, that is, the root mean square error (RMSE), the temporal correlation coefficient (TCC) and the spatial correlation coefficient (SCC) between observations and

simulations, are calculated in this study. The equations are written as:

$$\text{RMSE} = \sqrt{\frac{\sum(m_i - o_i)^2}{N_i}}, \text{ or } = \sqrt{\frac{\sum(m_t - o_t)^2}{N_t}}, \quad (1)$$

$$\text{TCC} = \frac{\sum(m_t - \bar{m}) \cdot \sum(o_t - \bar{o})}{\sqrt{\sum(m_t - \bar{m})^2 \cdot \sum(o_t - \bar{o})^2}}, \quad (2)$$

$$\text{SCC} = \frac{\sum(m_i - \bar{m}) \cdot \sum(o_i - \bar{o})}{\sqrt{\sum(m_i - \bar{m})^2 \cdot \sum(o_i - \bar{o})^2}}, \quad (3)$$

where m_i is the spatially averaged value from model outputs; o_i is the spatially averaged value from reanalysis/observations; m_t is the annually averaged value from the model outputs; o_t is the annually averaged value from reanalysis/observations; and N_i or N_t is the number of grid points or years.

Comparison is conducted on climate mean, seasonal cycle and interannual variations of surface temperature and precipitation. Interannual variability is expressed in terms of SD , which is derived from the time series of annual or seasonal mean variable on each grid. By comparing interannual variability of the observation and the models, the ability of models to reproduce the year-to-year variability of temperature or precipitation can be assessed. In addition, the seasonal cycle of temperature and precipitation averaged for each sub-region is also calculated to determine how well the RCMs capture the seasonality in each sub-region.

3 | RESULTS

In this section, the RCMs simulated surface air temperature, precipitation and large-scale circulation are compared with observation/reanalysis to evaluate the ability of RCMs to reproduce the regional climate over East Asia.

3.1 | Mean climatology

The general abilities of the RCMs to reproduce the mean surface climatology are firstly assessed by comparing the model simulations with the observations during the period of 1989–2009. Figure 2 presents annual, summer (June–July–August, JJA) and winter (December–January–February, DJF) mean surface air temperature from the gridded observation

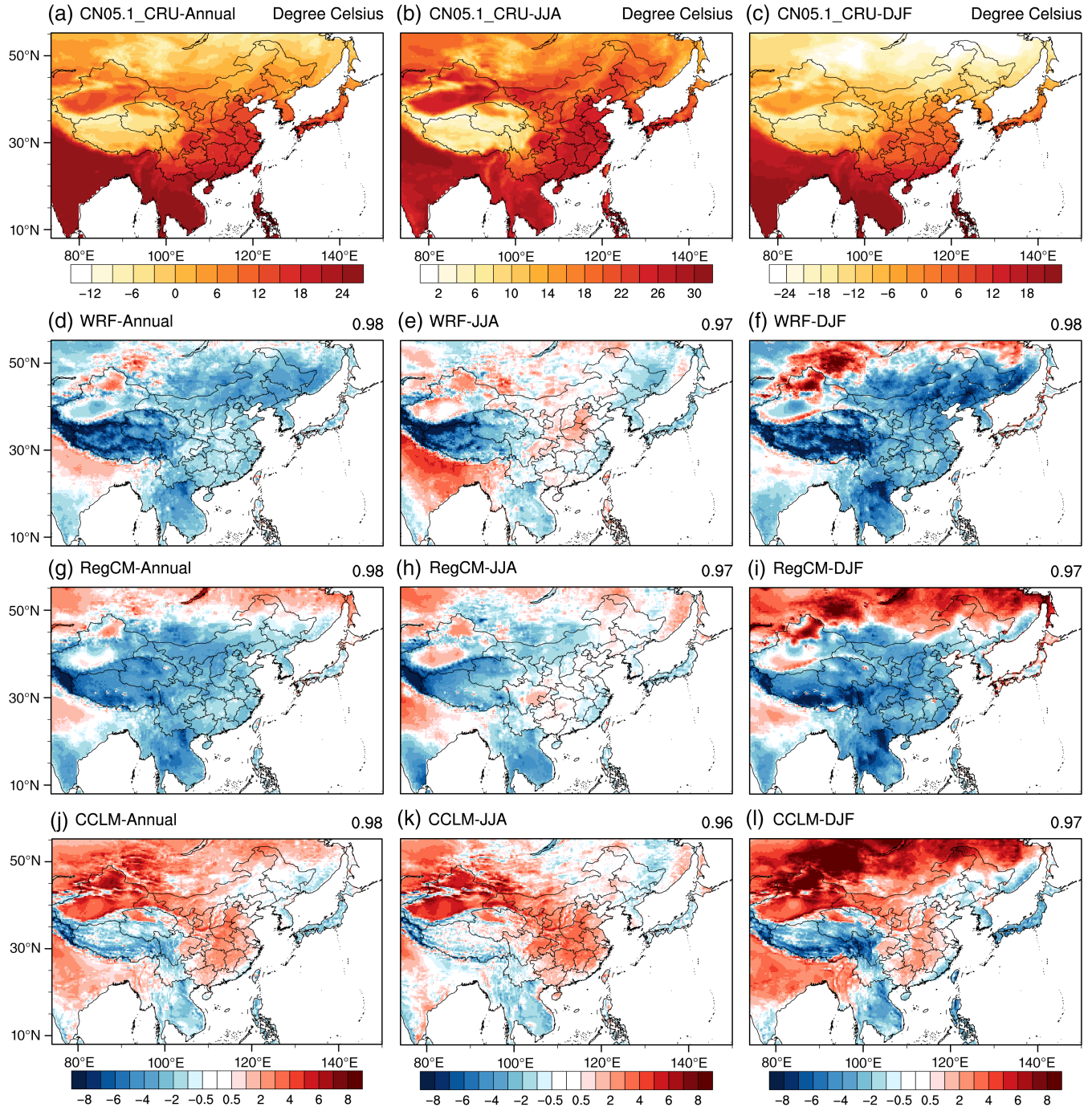


FIGURE 2 The 21-year (1989–2009) averaged annual and seasonal mean surface air temperature observation from CN05.1_CRU (a, b, c), and the differences between RCMs and CN05.1_CRU (d–l). The numbers appear in the upper right corner indicate the SCC

(CN05.1_CRU) and the biases between the RCMs simulations and the observation. The observed annual and seasonal mean surface air temperatures are both distributed as decreasing from the south to the north (Figure 2, first panel) with the maximum values over India and Indo-China Peninsula, while the spatial patterns of the biases between the RCMs outputs and CN05.1_CRU are quite different. For the annual mean surface air temperature, WRF and RegCM4 produce underestimations over most areas in China especially over Tibet Plateau (TP) with the maximum bias at about -8°C , while overestimations are found over northern India (Figures 2d,g). In summer (Figures 2e,h), WRF and RegCM4 can well simulate the surface air temperature over most regions in East Asia with biases ranging from -1 to $+1^{\circ}\text{C}$, but show clear cold bias over TP and warm bias over northern India. The winter temperature is evidently underestimated in the WRF and RegCM4 experiments over most areas in China (Figure 2f,i). In the CCLM simulation (Figure 2j-l), large warm biases exist over most areas in the domain, especially over the regions north of 40°N . Comparing the biases of the annual and seasonal temperatures, we can clearly find that the RCMs have relative poor performance in simulating the surface air temperature in cold seasons. The relatively larger bias in the winter time is possibly caused by the poor representation of land surface processes and the coherent bias from ERA-Interim reanalysis dataset (Ozturk *et al.*, 2012; Yu *et al.*, 2015). The comparison between WRF, RegCM4 and CCLM shows that RCMs with different dynamic core and physical parameterizations produce quite different spatial distributions of biases of surface air temperature in China. But all the three RCMs have cold biases over TP and warm biases over northern India, which may indicate that the complex topography over TP is important for the simulation of surface air temperature due to its physical and dynamical effects. The uncertainty of observation caused by sparse stations (Wu and Gao, 2013) is another reason for the common cold bias over TP.

Accurate representation of the spatial distribution of precipitation is critical for the applications of the regional climate modelling. Figure 3 shows the 21-year averaged annual, summer and winter precipitations from observation (CN05.1_GPCP) and the biases produced by different RCMs. Obviously, WRF, RegCM4 and CCLM can well reproduce annual mean precipitation over most land areas in East Asia, with the biases ranging from -2 to $+2 \text{ mm/day}$. However, large wet biases exist over ocean especially in the WRF simulation, which has maximum wet biases above 6 mm/day over western Pacific, and CCLM agrees well with the observation over ocean. In East Asia, the total precipitation amount is mainly contributed by the summer monsoonal precipitation. It is clear that the spatial patterns of the summer precipitation biases are quite similar with those of the annual precipitation. But the magnitudes of the summer precipitation biases are

about twice larger than that of annual mean. There are some differences of the annual and summer precipitation biases among the three RCMs. WRF tends to underestimate precipitation over most land areas but obviously overestimate it over ocean. RegCM4 exhibits wet biases over most land areas except for East China and northern India. CCLM shows similar distribution of precipitation biases as WRF, except that it produces larger wet biases over TP. The precipitation biases in winter are relatively small (Figure 3f,i,l), and WRF and RegCM4 show similar spatial distributions with wet biases over most regions in the domain except southeastern China. As opposed to WRF and RegCM4, CCLM has negative biases over regions south of 20°N .

Taylor diagrams (Taylor 2001) provide a visual framework to access the performances of the models in simulating the spatial distributions of annual or seasonal mean variables, consisting of *SD*, RMSE and correlation between models and the reference observations. Figure 4 demonstrates the Taylor diagrams for the spatial distributions of the annual and seasonal mean temperature and precipitation over China mainland (CN) and the whole domain. For the surface air temperature, all the three RCMs can well simulate the spatial patterns with high correlation coefficients (>0.92), but overestimate the spatial variability especially in winter over China mainland. For the precipitation, the spatial correlations are ranging from 0.5 to 0.9, and the correlations over China mainland are higher. The CCLM model can reproduce the spatial patterns and variability of precipitation over East Asia, while WRF significantly enlarge the spatial variability with the ratio of *SD* reaching 2.5. RegCM4 skillfully simulates the spatial patterns of precipitation over China Mainland, but clearly overestimates the spatial variability over East Asia, especially in summer.

3.2 | Interannual variations

To assess the performance of the RCMs in simulating the interannual variations of surface air temperature and precipitation, the temporal correlations (TCORs) and RMSEs are calculated between the model simulations and observation at each grid. Figure 5 shows the spatial distributions of the TCOR and RMSE for the annual mean surface air temperature. Obviously, the interannual variations of the temperature are well captured by the three RCMs with the correlation coefficients exceeding 0.60 over most regions in East Asia. However, WRF demonstrates low correlations below 0.3 over west area of the Tibetan Plateau and part of North China (NC) and South China (SC), which are not significant at the 0.95 confidence level. RegCM4 produces relatively lower correlations over Northeast China (NEC), Tibetan Plateau (TP) and south of the Indian Peninsula. Among the three RCMs, CCLM shows the best

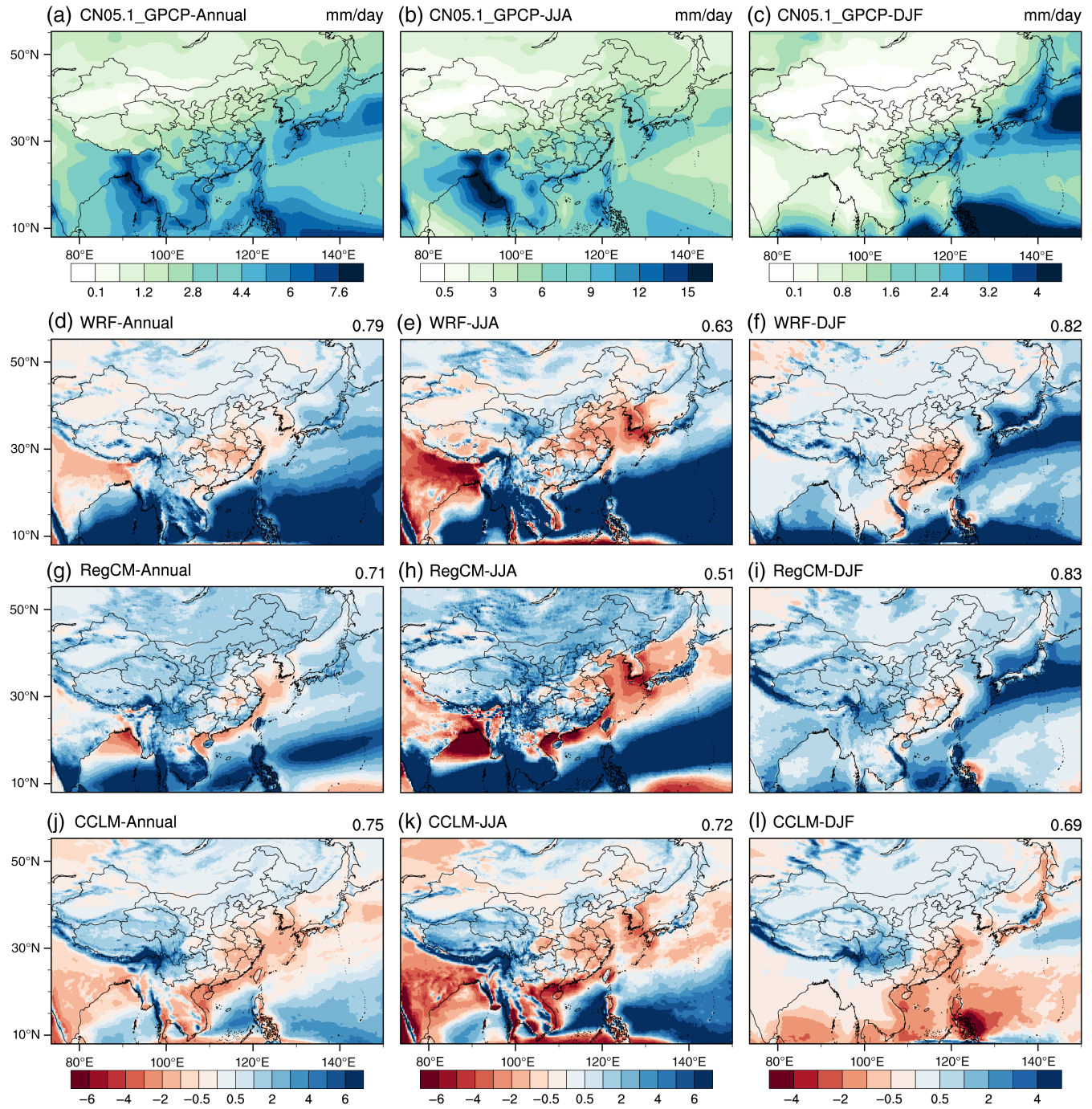


FIGURE 3 The same as Figure 2, but for annual and seasonal mean precipitation and the observation data is CN05.1_GPCP

performance in reproducing the interannual variability of the surface air temperature, with the TCORs higher than those in the other two RCMs especially over Northeast China, central China and the Tibetan Plateau. As shown in Figure 5b,d, the spatial patterns of the RMSE from WRF and RegCM4 simulations are quite similar, with the largest RMSEs over the Tibetan Plateau, and WRF shows relative large RMSEs over Northeast China. Compared to WRF and RegCM4, CCLM generates much lower RMSEs over

most areas in the domain, especially over the Tibetan Plateau and Indo-China peninsula.

Figure 6 depicts the distributions of TCORs and RMSEs of the annual mean precipitation. It is clear that the TCORs of precipitation are much lower than those of temperature. WRF and RegCM4 cannot reasonably capture the interannual variations of precipitation over South China (SC), Indo-China peninsula and the western North Pacific (WNP), where most of the correlations are below 0.3. CCLM

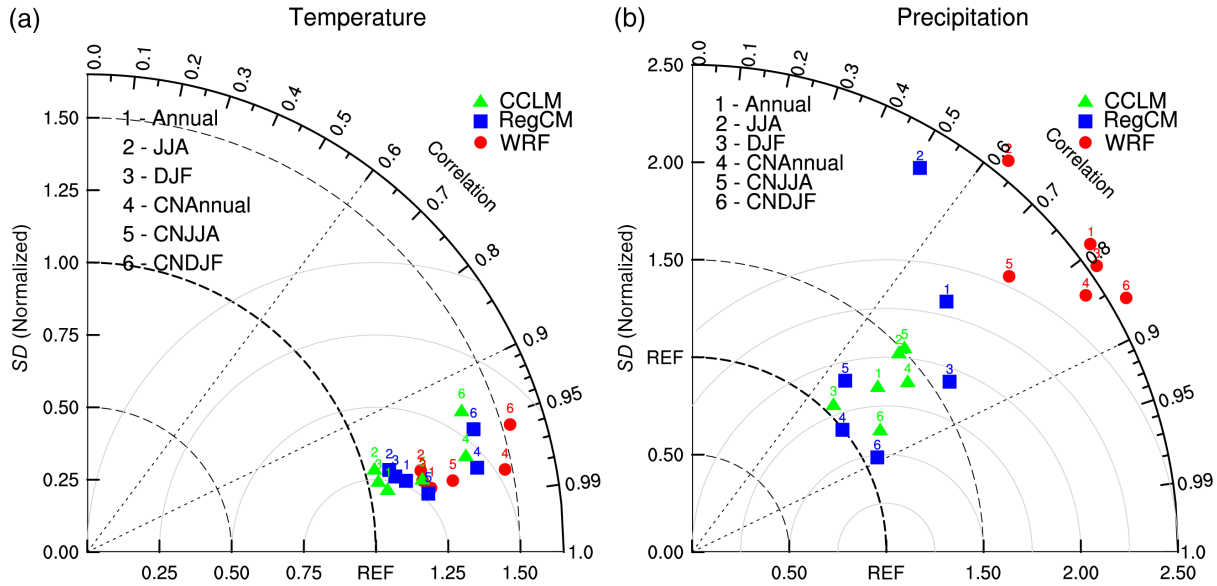


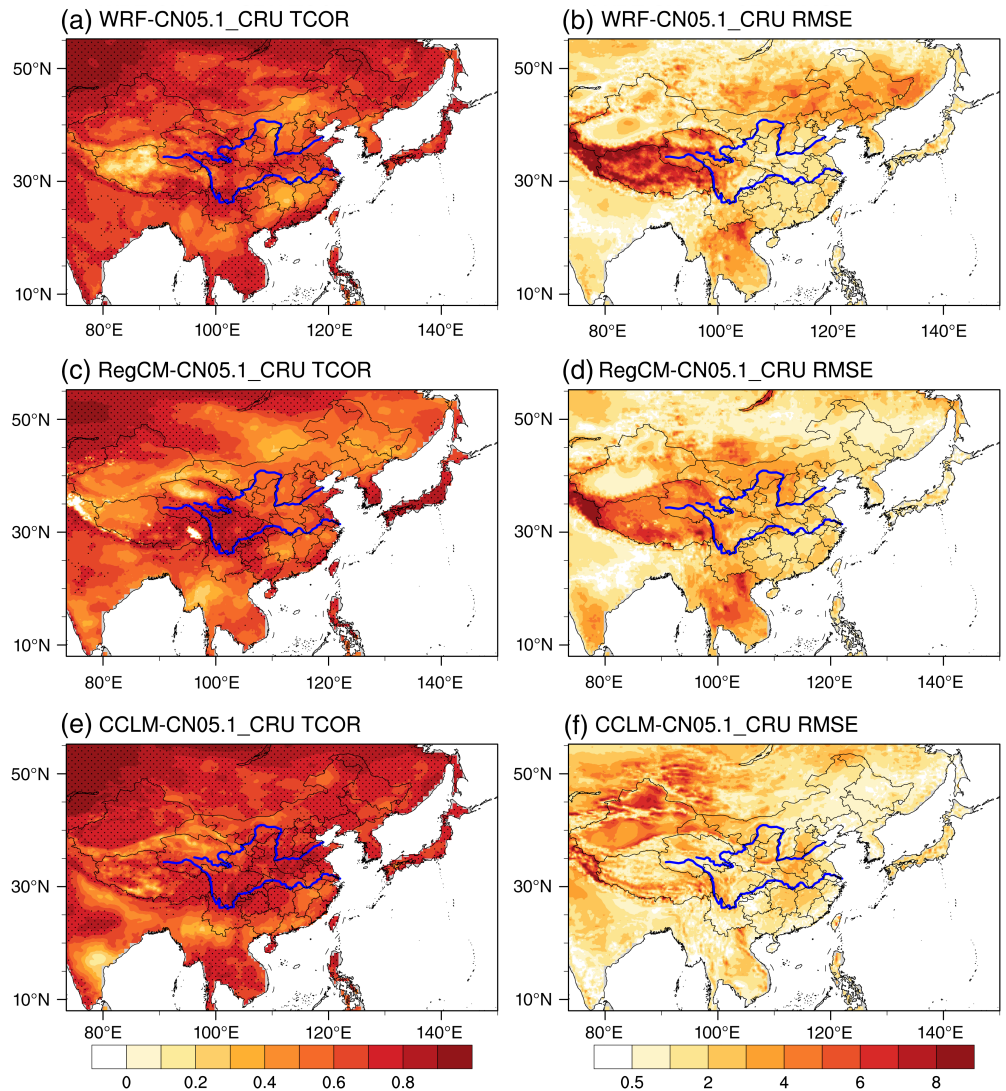
FIGURE 4 Taylor diagram for the annual and seasonal mean surface air temperature and precipitation simulated by three RCMs in the seven sub-regions. The radial distance from the origin represents the ratio between the simulated and observed SD of the temperature and precipitation averaged during 1989–2009. The azimuthal position gives the SCC between the simulation and observation. The distance from the REF point demonstrates the normalized centered RMSE

outperforms the other two RCMs over most regions in China with most of the correlations above 0.3. The TCCs over some regions are even negative. The unreal representation of ocean–atmosphere interaction, the related teleconnections and the low-level circulations in the RCMs may lead to the deficiency in capturing the interannual variability of precipitation over the boundary between the East Asian summer monsoon and the western North Pacific summer monsoon, which have a well-known dipole interannual mode (Park *et al.*, 2013; Song and Zhou, 2014). We can infer that the RCMs cannot separate the two monsoon systems reasonably. The RMSEs produced by the WRF model are below 2.0 mm/day over most land areas, but are apparently higher over regions south of 20°N, especially over the tropical ocean region with RMSE exceeding 7 mm/day. RegCM4 generates larger RMSEs than WRF over most land areas, especially over central China, northern China and Mongolia, where the RMSEs exceed 2.5 mm/day. But it reduces the RMSEs over ocean compared to WRF. CCLM performs best by giving the RMSEs below 2.5 mm/day in most regions in East Asia, especially over the ocean regions where the RMSEs are much larger in the WRF and RegCM4 simulations.

To further evaluate the ability of the three RCMs to reproduce the interannual variations over different sub-regions, regional averaged annual mean temperature and precipitation simulated by RCMs are compared with the observations. The TCORs and RMSEs of the interannual variations of annual mean surface temperature and precipitation between the RCM simulations and observations are calculated at each sub-region, and are shown as Taylor

Diagram in Figure 7. For temperature (Figure 7a), it can be found that CCLM outperforms the other two RCMs with the TCORs above 0.7, which are higher than those in WRF and RegCM4. And WRF also has better performance in reproducing the regional averaged interannual variations of temperature than RegCM4 over most sub-regions. CCLM and WRF tend to enlarge the temperature variability over Northeast China and India, while RegCM4 will weaken it over South China and Indo-China Peninsula. For precipitation (Figure 7b), the RCMs show quite different performances in simulating its interannual variations. CCLM can well simulate the interannual variations of annual mean precipitation over North China, Northeast China, Northwest China and Indo-China Peninsula with the TCORs above 0.5, but it fails to produce the interannual variability of precipitation over South China and India with the TCORs below 0.2. Meanwhile, the TCORs simulated by WRF and RegCM4 are below 0.4 in most sub-regions except in Northwest China, which means that WRF and RegCM4 have lower abilities to simulate the interannual variations of precipitation. Over different sub-regions, the RCMs also have quite different capabilities to produce the variability. WRF and CCLM have higher skills over North China, Northeast China and Northwest China, but lower performances over South China, Yangtze-Huaihe River basin and India where the precipitation is clearly affected by the East Asia monsoon system. However, RegCM4 shows similar skills in producing the precipitation variability over different sub-regions. All the three RCMs tend to overestimate the interannual variability over most sub-regions.

FIGURE 5 The temporal correlation (TCOR) coefficient and RMSE of annual temperature for each grid point between RCMs and CN05.1_CRU, the black dots indicate the areas with correlations significant at the 0.95 confidence level



3.3 | Annual cycle

The annual cycles of surface air temperature averaged over the sub-regions are shown in Figure 8. Overall, all the three RCMs can approximately reproduce the seasonal cycles of surface air temperature over all the sub-regions with the temporal correlations above 0.97 (Table 2). The observed precipitation peaks in July in most sub-regions, except India and Indo-China where the peaks show up in May and April. The RCMs can simulate the peaks over most sub-regions except Indo-China, where CCLM can reproduce the seasonal cycle but WRF and RegCM4 show the peaks in June which postpone for 2 months. In SC, YHR, NC and NWC (Figure 8a–c,e), it is clear that large warm biases exist in the CCLM simulations especially in warm seasons and can reach 3°C. In YHR (Figure 8b), large cold biases can be found in WRF and RegCM4 simulations in cold seasons with the largest biases exceeding 3°C. In NEC (Figure 8d), the annual cycles of surface air temperature simulated by CCLM and RegCM4 are close to the observation with the

RMSEs below 2.1°C, while WRF underestimates the temperature during winter and spring with the RMSE exceeding 3.6°C. Among the three RCMs, only CCLM can reproduce the seasonal cycle of temperature over Indo-China Peninsula with the RMSE below 1.2°C. WRF generates large cold biases in cold seasons with the RMSE above 2.5°C, while RegCM4 underestimates the surface air temperature during the whole year with the RMSE reaching 3.2°C.

Figure 9 demonstrates the simulated and observed seasonal cycles of precipitation over different sub-regions on land area. All the three RCMs can simulate the annual cycles of precipitation with the correlations above 0.92, but obvious differences can be found over different regions for different RCMs. Over South China, the observed seasonal cycle of precipitation has two peaks in June and August. CCLM can well reproduce the cycle and the two peaks but underestimate the precipitation, while WRF and RegCM4 only simulate one peak in July and tend to overestimate the precipitation in warm seasons. RegCM4 shows best performance to simulate

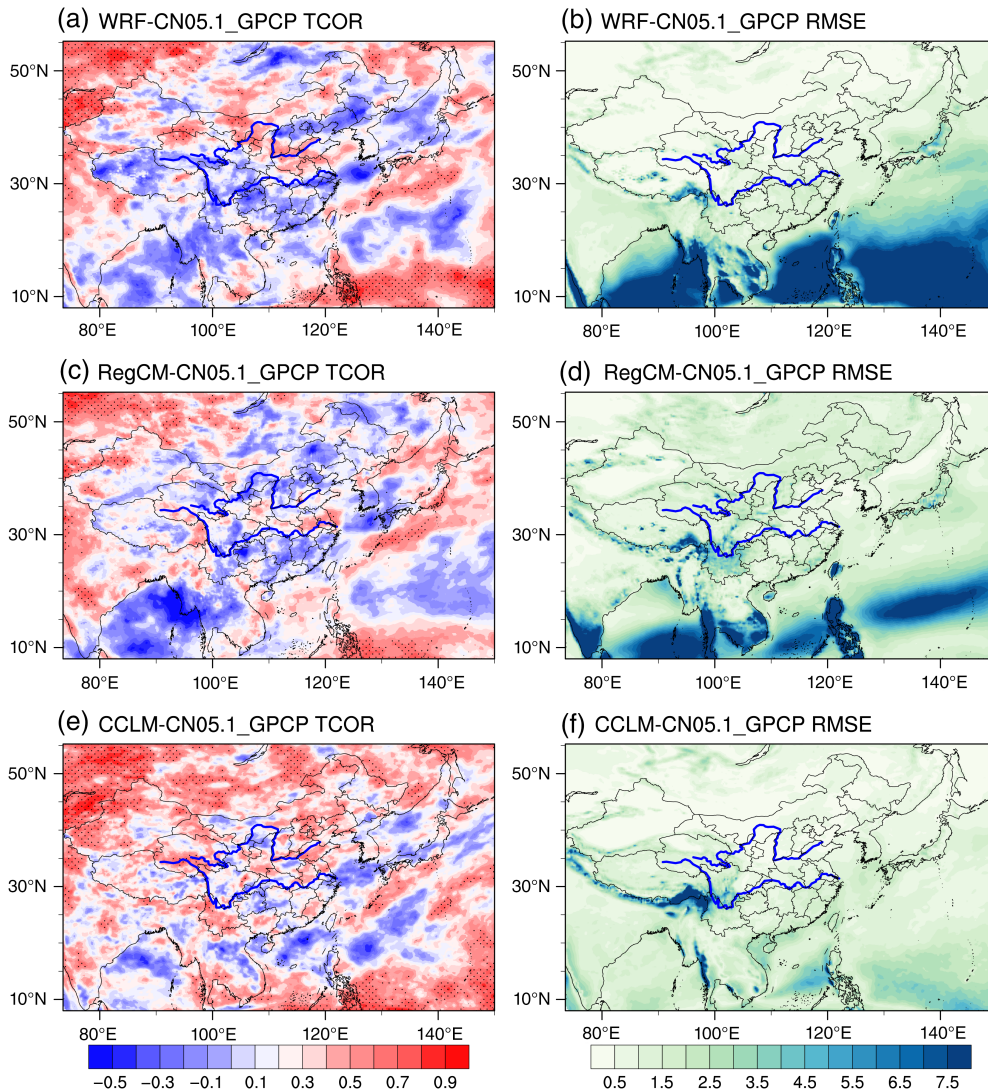


FIGURE 6 The same as Figure 5, but for precipitation, and the observation data is CN05.1_GPCP

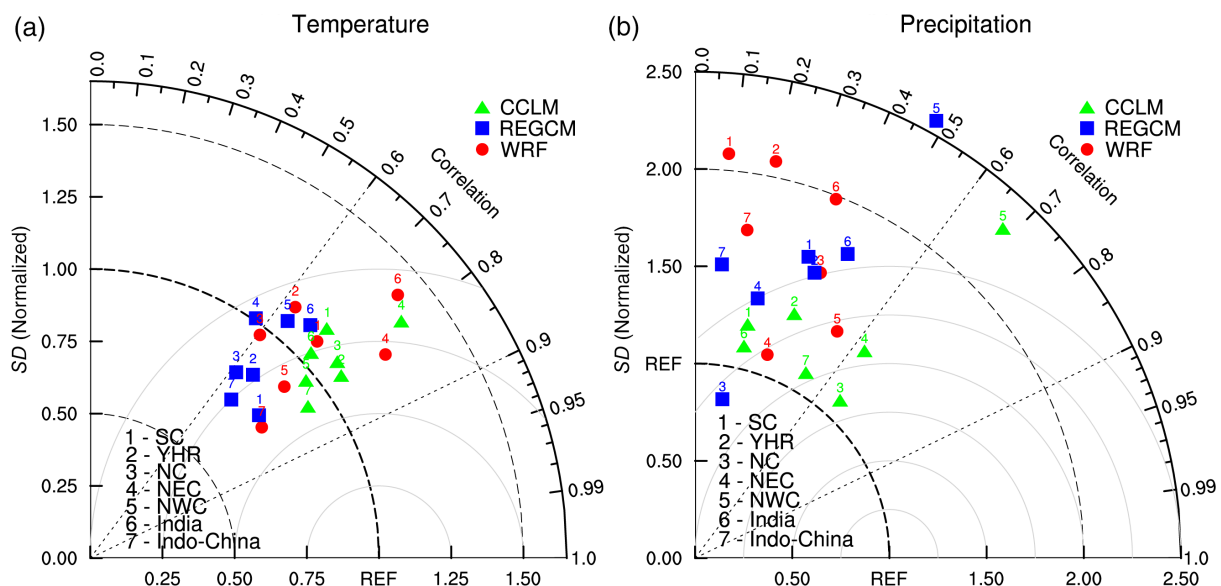


FIGURE 7 Taylor diagrams for the inter-annual variations of the regional averaged temperature and precipitation

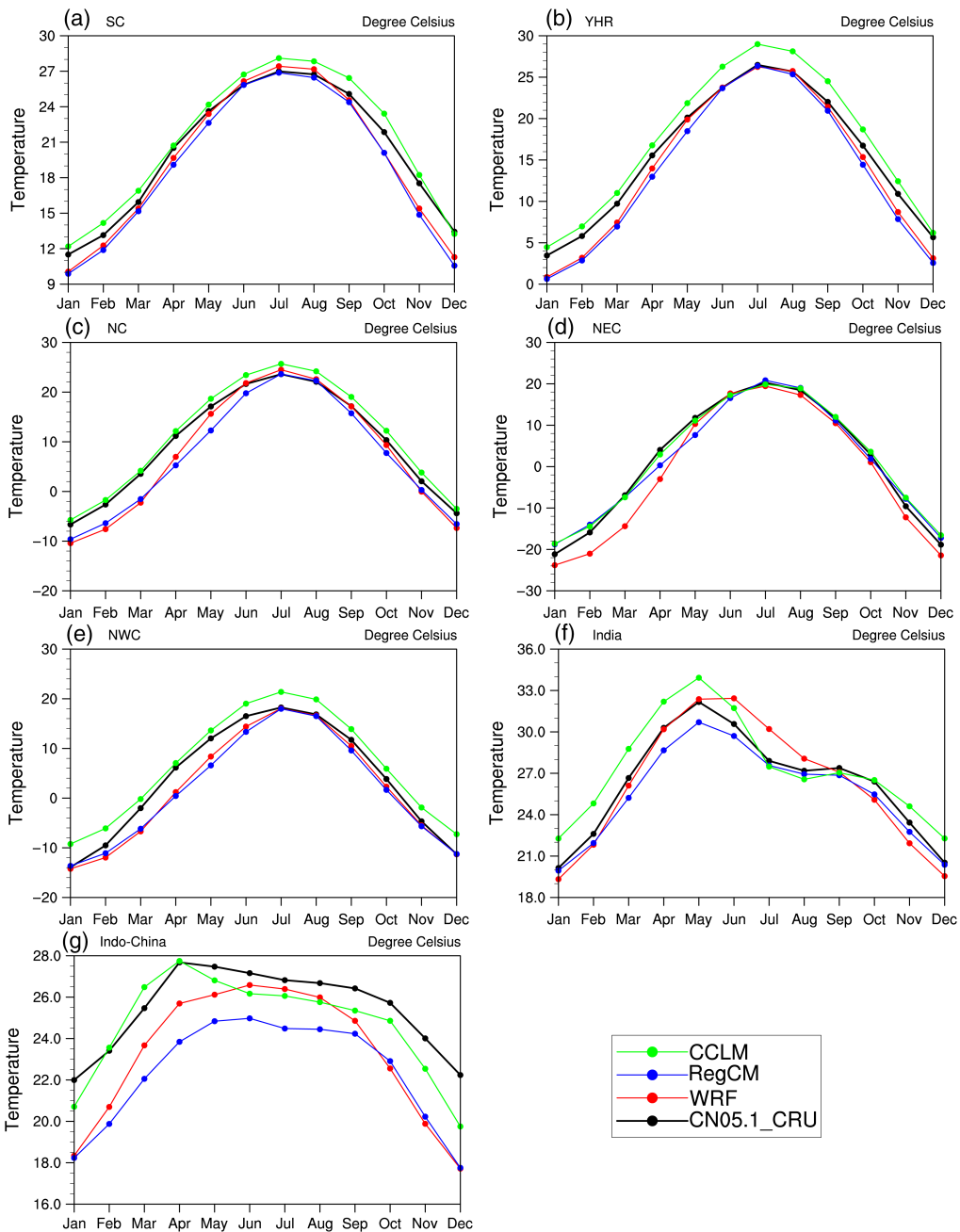


FIGURE 8 The annual cycles of temperature in each sub-region (land only)

the annual cycle of precipitation over Yangtze-Huaihe River basin with the correlation at 0.98 and RMSE at 0.68 mm/day. CCLM also reproduce the cycle but underestimates the precipitation. WRF produces the peak of the monthly precipitation over YHR in August, which is 2 months later than that in the observation. Over the northern regions in China (NC, NEC and NWC) and India (Figure 9c–e), the RCMs can simulate the seasonal cycles of precipitation with the peaks close to the observations and the correlations above 0.92, but RegCM4 clearly overestimates the precipitation especially in warm seasons with the RMSEs all above 1.1 mm/day and even reaching 2.8 mm/day in India. Among the three RCMs,

the seasonal cycle of precipitation simulated by CCLM is closest to the observation over Indo-China Peninsula (Figure 9g), and the RMSE is at about 1.5 mm/day; while large wet biases can be found in WRF and RegCM4 simulations with the RMSEs above 5.0 mm/day.

Figure 10 shows the simulated and observed zonal mean ($105\text{--}120^\circ\text{E}$) precipitation (land only) in each month during the period of 1989–2009. It can be found that the time of peak precipitation varies with latitude, which is inseparable from the propagation of monsoon precipitation. All the three RCMs can basically simulate the propagation of precipitation with latitude, but obvious biases exist. Over regions

T_2 m	WRF		RegCM		CCLM	
	CORR	RMSE	CORR	RMSE	CORR	RMSE
SC	0.99	1.19	0.99	1.5	0.99	0.95
YHR	0.99	1.71	0.99	2.22	0.99	1.82
NC	0.99	2.99	0.99	3.25	0.99	1.54
NEC	0.99	3.67	0.99	2.03	0.99	1.32
NWC	0.99	2.5	0.98	2.92	0.99	2.87
India	0.98	1.08	0.99	0.82	0.96	1.48
Indo-China	0.97	2.59	0.98	3.19	0.95	1.15
Precipitation	CORR	RMSE	CORR	RMSE	CORR	RMSE
SC	0.95	1.37	0.98	1.46	0.98	1.35
YHR	0.95	0.82	0.98	0.68	0.95	0.75
NC	0.98	0.29	0.93	1.46	0.98	0.29
NEC	0.99	0.4	0.96	1.49	0.96	0.57
NWC	0.93	0.24	0.96	1.11	0.93	0.57
India	0.94	1.35	0.99	2.84	0.98	1.53
Indo-China	0.97	6.58	0.98	4.99	0.96	1.47

TABLE 2 The TCOR and the RMSE of annual cycle of temperature and precipitation between RCMs and the observation in each sub-region

south of 20°N, the RCMs all present poor performance in simulating the peak precipitation in August and September. WRF evidently overestimates the precipitation over regions south of 20°N during May, June and July. Meanwhile, RegCM4 and CCLM both generate an unreal pattern that has two precipitation peaks in May (June) and September, respectively. Over the regions between 22°N and 30°N, the observed zonal mean precipitation peaks in June. CCLM has the ability to reproduce the precipitation propagation over these regions but underestimates the precipitation intensity, while the peak precipitation produced by WRF and RegCM4 appears in June and July. WRF and CCLM approximately reproduce the precipitation pattern over northern regions above 30°N, while RegCM4 obviously overestimates the precipitation systematically and simulates the peak precipitation 1 month earlier than that of the observation.

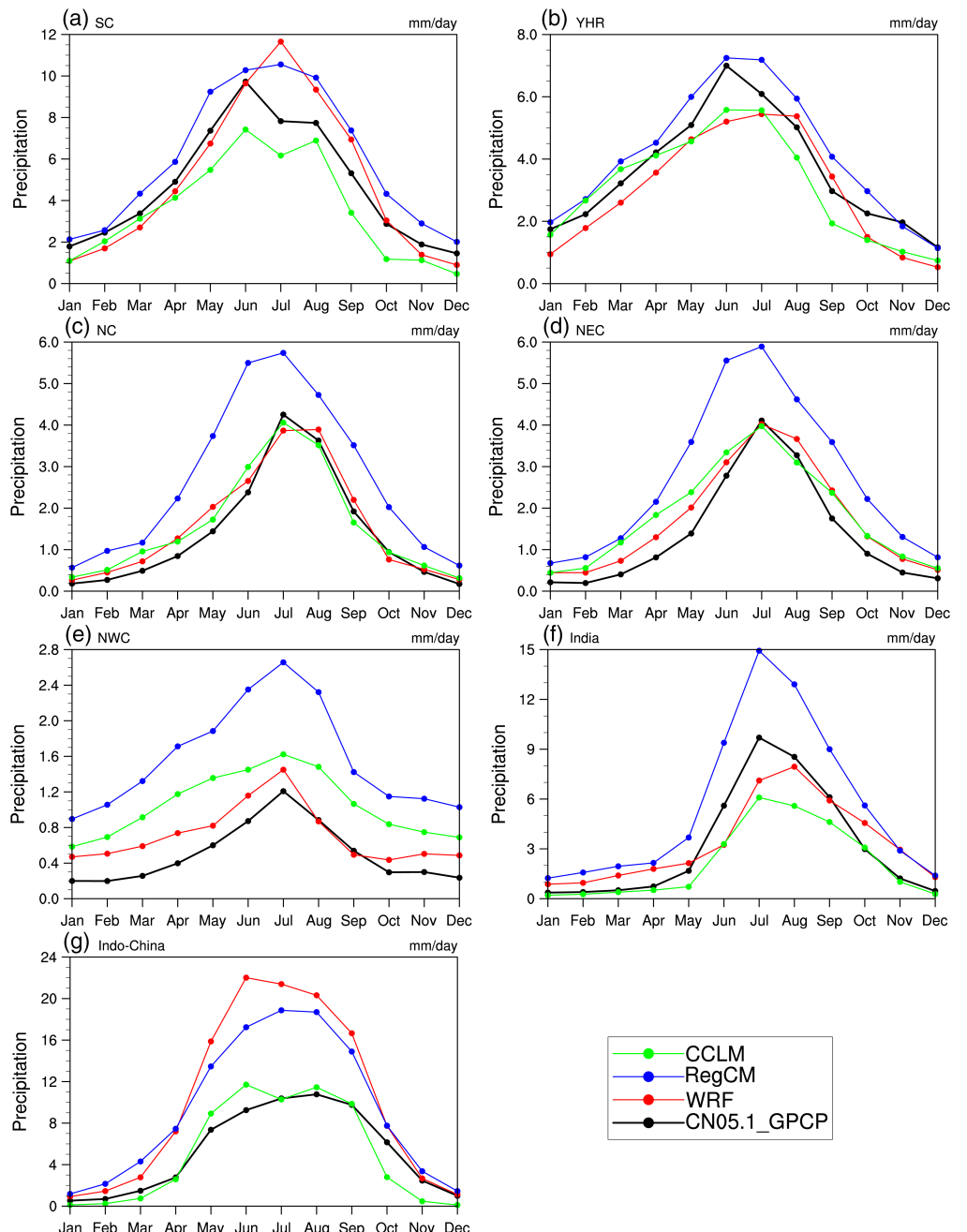
3.4 | Circulations

To assess how the RCMs simulate the atmospheric circulation, we calculate the annual and seasonal mean biases of wind field and specific humidity at 850 hPa level between the RCM simulations and the ERA-Interim reanalysis dataset (Figure 11). The reanalysed specific humidity increases from north to south, and the main centres of water vapour convergence locate at northern India, Indo-China Peninsula and northern equatorial western Pacific. All the RCMs can reasonably capture the spatial patterns of specific humidity at low levels with spatial correlations above 0.9 and RMSEs below 1.3 g/kg (not shown). WRF and RegCM4

show quite similar biases of specific humidity and winds at 850 hPa between simulations and reanalysis. Dry biases can be found over eastern China and northern India which may cause the dry biases of precipitation especially in summer (Figure 3). And large wet biases exist over western Pacific with cyclonic circulation anomalies at low level in summer, which is consistent with the large positive precipitation biases over there. In the CCLM simulation, the biases of precipitation decrease with the reduction of specific humidity biases over western Pacific in summer, and the dry biases of precipitation over western Pacific in winter are mainly caused by the negative biases of specific humidity. Although the biases of specific humidity in CCLM are lower than those in WRF and RegCM4 over eastern China and northern India, the dry biases of precipitation increase over there, which means that precipitation is also controlled by other factors, such as land-atmosphere interaction and convection parameterization, besides the water vapour and circulation.

To further evaluate the RCMs' performance on simulating the interannual variations of mid-level atmospheric circulation, the correlations of interannual variations of geopotential height at 500 hPa (abbreviated to H500) between the RCM simulations and ERA-Interim reanalysis are calculated at each grid and shown in Figure 12. It can be found that CCLM better simulates the interannual variability of H500 with the temporal correlations above 0.70 over most regions (Figure 12c). And the temporal correlations in the CCLM simulation are higher than those in WRF and RegCM4, which is consistent with the relative better simulation of the interannual variations of precipitation over the

FIGURE 9 The same as Figure 8, but for precipitation (land only)



CORDEX East Asia. In the WRF and RegCM4 simulations (Figure 12a,b), low temporal correlation centres can be found over western Pacific, which is associated with the poor simulations of interannual variations of precipitation over there.

4 | CONCLUSIONS

In this study, three RCMs, namely, WRF, RegCM4 and CCLM, are evaluated against the observational datasets including CN05.1, CRU and GPCP to examine how skillful they are in simulating the key features of the regional climate over CORDEX-EA-II domain.

The RCMs have the capability of simulating the annual and seasonal mean surface air temperature and precipitation, however, some biases are produced by the models. For the annual and seasonal mean temperature, WRF and RegCM4 exhibit underestimations over most areas in China, especially over the Tibet Plateau with the maximum bias at about -8°C . In contrast, CCLM generally overestimates the annual and seasonal mean temperatures over the whole domain except over the Tibetan Plateau and Indo China. All the three RCMs have poorer performances in simulating the winter temperature. In addition, other factors like the complex topography and the different dynamic cores and physical parameterizations of the RCMs may lead to quite

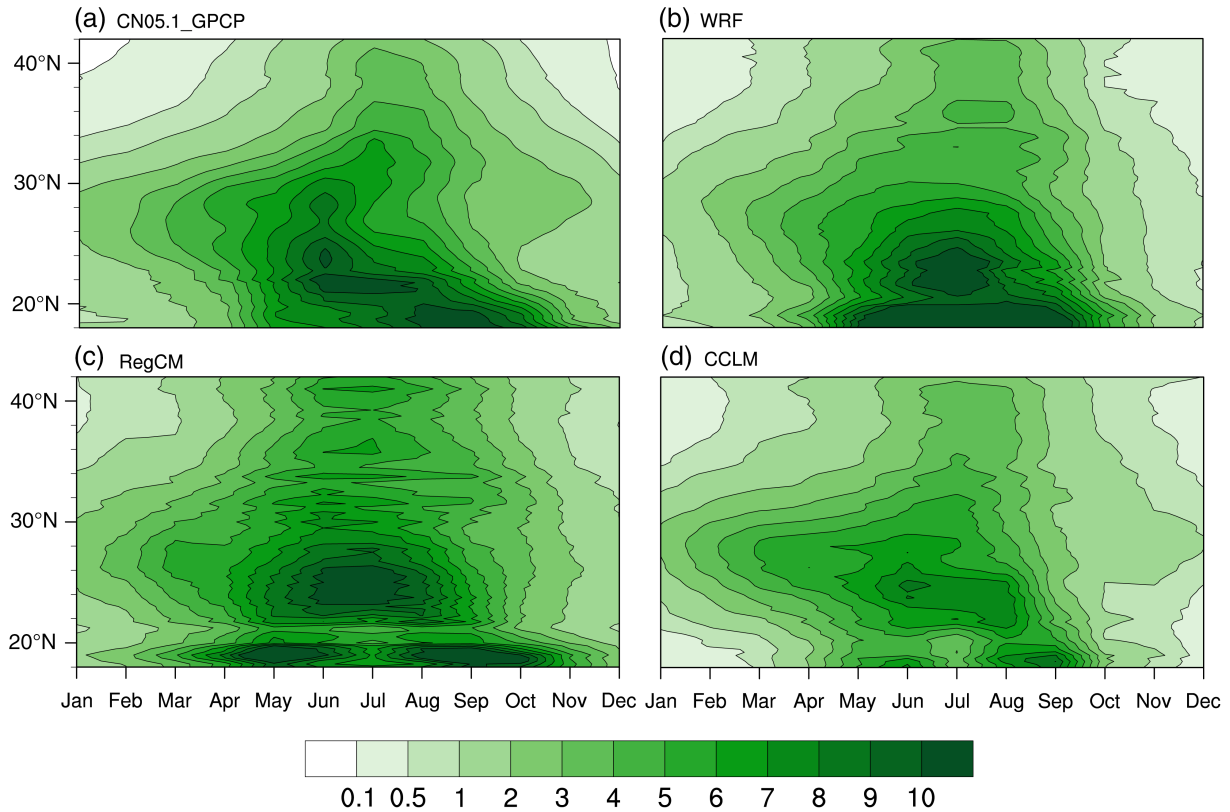


FIGURE 10 Hovmöller diagrams of the observed (a) and simulated (b–d) precipitation annual cycle over Eastern China (105° – 120° E). Units: mm/day

different spatial distributions of biases. The annual and seasonal precipitations are generally overestimated over the Tibetan Plateau and Northeast China, while underestimated in East China. In addition, large wet biases exist over ocean especially in the WRF simulation, and CCLM agrees better with the observation over ocean. It is known that the Kain-Fritsch convection parameterization scheme applied in WRF and the MIT scheme applied in RegCM4 tend to generate systematic positive biases of monsoon westerly and convection precipitation, as well as extended rainband over WNP (Chow *et al.*, 2006; Cha *et al.*, 2011; Zou *et al.*, 2014; Cha *et al.*, 2016). Too strong low-level southwesterly winds and the Somalia Jet in JJA and large biases of moisture produced by the RCMs lead to the difficulty in simulating the mean precipitation.

The RCMs' ability to simulate the interannual variations of the surface air temperature and precipitation is also evaluated against the observation. It is clear that the interannual variation of the temperature is much better reproduced than that of the precipitation. In general, CCLM outperforms WRF and RegCM4 in simulating the interannual variations of temperature, especially in NC, YHR and TP. WRF and RegCM4 also have poor performances in capturing the interannual variations of precipitation over SC, Indo-China peninsula and WNP. The better presentation of the inter-annual

variation of H500 in the CCLM simulation results in the relative better simulation of the interannual variation of precipitation in the domain. In addition, the exclusion of air-sea coupling in WRF and RegCM4, which is crucial to the simulation of the interannual variability of summer rainfall over Southeast China, South China Sea and WNP (Zou and Zhou, 2013), can also result in the poor performance.

Generally, all the three RCMs can well reproduce the seasonal cycles of the surface air temperature over most sub-regions except in Indo-China, where CCLM can demonstrate the seasonal cycle but WRF and RegCM4 show the temperature peaks postponed for 2 months. CCLM tends to overestimate the temperature especially in warm seasons, while cold biases occur in the simulations of WRF and RegCM4. Overall, CCLM outperforms the other two RCMs with lowest RMSEs in most sub-regions. For the annual cycle of precipitation, the performances of the RCMs are inferior to those for the temperature. Only in the northern regions of China can all the three RCMs well reproduce the precipitation peaks. CCLM has a close agreement with the observation over Indo-China Peninsula, while WRF and RegCM4 produce large wet biases.

The simulated and observed zonal mean (105° – 120° E) precipitation (land only) in each month is investigated to assess the models' ability to capture the moving of rain

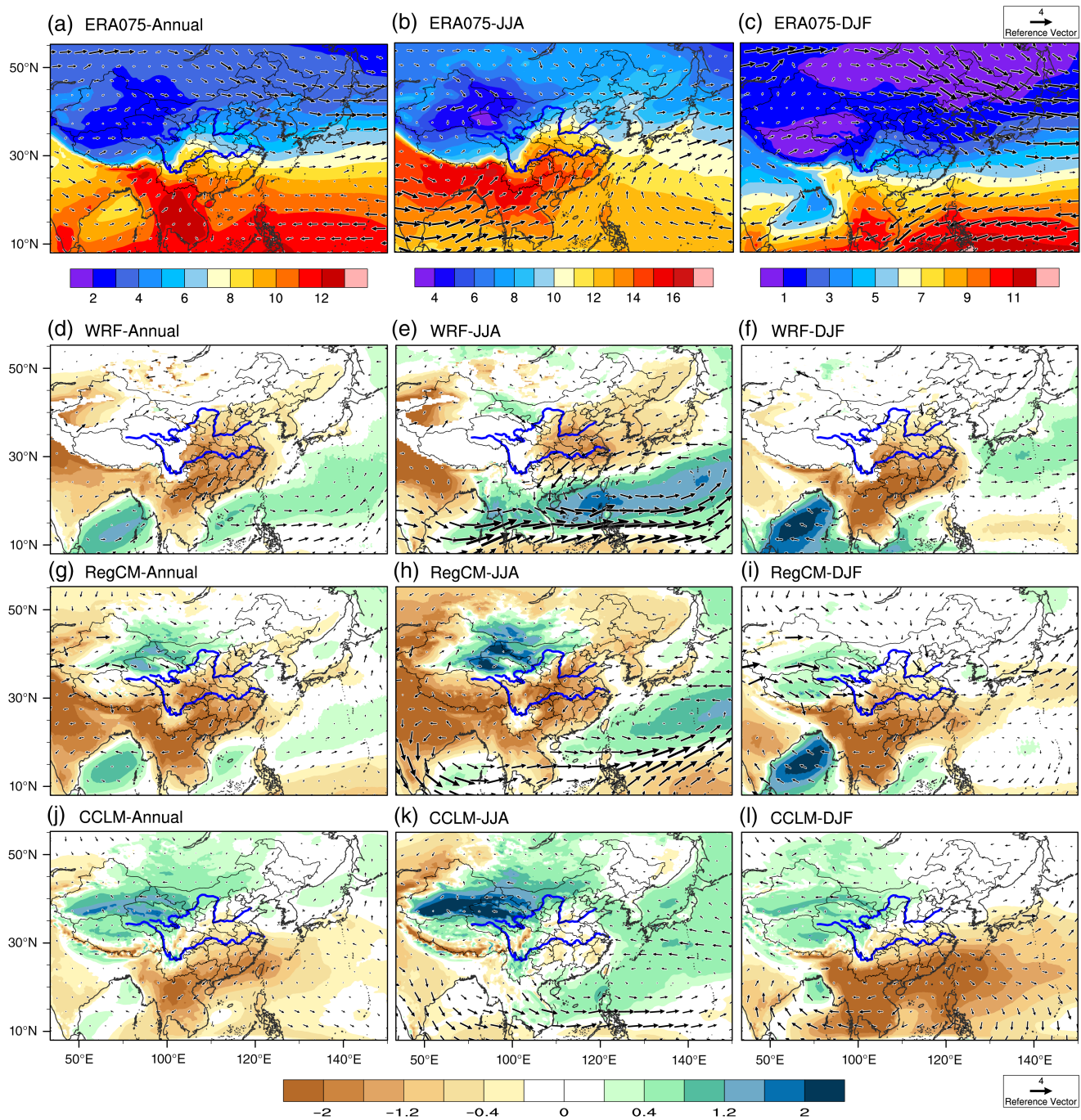


FIGURE 11 Seasonal mean specific humidity (shading, units: g/kg) and wind field (arrow, units: m/s) at 850 hPa. The first row (a–c) represents the ERA-interim reanalysis, and second to fourth rows (d–f, g–i, j–l) represent the differences between WRF, RegCM4, CCLM and the ERA-interim reanalysis, respectively

belt in East China. All the three RCMs have the ability to simulate the variations of precipitation with latitude and time. However, they all present poor performance over the regions south of 20°N. CCLM can well reproduce the precipitation peak through summer between 22° and 30°N in spite of underestimated intensity, while WRF and RegCM4 fail to capture the peak time of the precipitation. Over the regions north of 30°N, WRF and CCLM approximately reproduce the precipitation pattern, while

RegCM4 has systematic positive biases and earlier precipitation peak.

The systematic biases of temperature and precipitation appear in regions with complex topography (i.e., TP) may be contributed by the uncertainty of the gridded observational dataset, which is interpolated from few observation stations. Over TP, the CN05.1 dataset is interpolated from sparse stations and tends to overestimate temperature. Previous studies have put forward various possible causes that

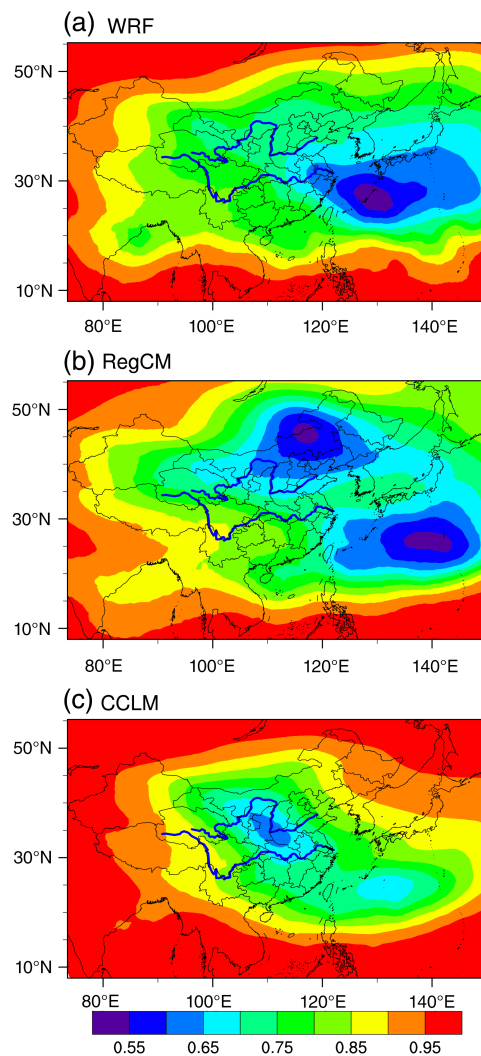


FIGURE 12 Spatial distributions of TCCs between the simulated and observed inter-annual variations of the geopotential height at 500 hPa

influence the simulation of surface climatology, including the choosing and updating of land surface model, cumulus convection parameterizations, model orography, etc. The application of spectral nudging (i.e., Tang *et al.*, 2017), air-sea coupling in RCMs (i.e., Yao and Zhang, 2010; Zou *et al.*, 2016) and ensemble averages of multi-RCM (i.e., Kim *et al.*, 2014) can improve the model performance efficiently. Last but not least, higher spatial resolution dependent on more computing resources would add value in dynamical downscaling. Additional analysis is underway to deepen the understanding of regional climate modelling and contribute to the development of latest RCM.

ACKNOWLEDGEMENTS

This work is jointly funded by the National Key Research and Development Program of China (2018YFA0606003,

2016YFA0600303) and the National Natural Science Foundation of China (41875124). The authors acknowledge with thanks the ECMWF for providing the ERA-interim reanalysis data as driving fields in the simulations, and Climate Research Unit (CRU) and Global Precipitation Climatology Project (GPCP) for providing the observation dataset. We also thank Dr. Jia Wu from the National Climate Center (NCC) of China Meteorological Administration (CMA) for providing the CN05.1 gridded dataset.

CONFLICT OF INTEREST

The authors declare no potential conflict of interest.

ORCID

Jianping Tang <https://orcid.org/0000-0002-1098-2656>

REFERENCES

- Adler, R.F., Huffman, G.J. and Chang, A. (2003) The version-2 global precipitation climatology project (GPCP) monthly precipitation analysis (1979-present). *Journal of Hydrometeorology*, 4(6), 1147.
- Baldauf, M., Seifert, A., Förstner, J., Majewski, D. and Raschendorfer, M. (2011) Operational convective-scale numerical weather prediction with the COSMO model: description and sensitivities. *Monthly Weather Review*, 139(12), 3887–3905. <https://doi.org/10.1175/MWR-D-10-05013.1>.
- Cha, D.H., Jin, C.S., Lee, D.K. and Kuo, Y.H. (2011) Impact of intermittent spectral nudging on regional climate simulation using weather research and forecasting model. *Journal of Geophysical Research*, 116(D10103).
- Cha, D.H., Jin, C.S., Moon, J.H. and Lee, D.K. (2016) Improvement of regional climate simulation of East Asian summer monsoon by coupled air-sea interaction and large-scale nudging. *International Journal of Climatology*, 36(1), 334–345.
- Chen, F. and Dudhia, J. (2001) Coupling an Advanced Land Surface-Hydrology Model with the Penn State–NCAR MM5 Modeling System. Part I: Model Implementation and Sensitivity. *Monthly Weather Review*, 129, 569–585.
- Chow, K.C., Chan, J.C.L., Pal, J.S. and Giorgi, F. (2006) Convection suppression criteria applied to the MIT cumulus parameterization scheme for simulating the Asian summer monsoon. *Geophysical Research Letters*, 33(24), 194–199.
- Christensen, J.H., Hewitson, B., Busuioc, A., Chen, A., Gao, X., Held, I., Jones, R., Kolli, R.K., Kwon, W.T., Laprise, R., Magaña Rueda, V., Mearns, L., Menéndez, C.G., Räisänen, J., Rinke, A., Sarr, A. and Whetton, P. (2007) Regional climate projections. In: Solomon, S., Qin, D., Manning, M., Chen, Z., Marquis, M., Averyt, K.B., Tignor, M. and Miller, H.L. (Eds.) *Climate Change 2007: The Physical Science Basis. Contribution of Working Group I to the Fourth Assessment Report of the Intergovernmental Panel on Climate Change*. Cambridge, UK and New York, NY: Cambridge University Press.
- Christensen, J.H., Machenhauer, B., Jones, R.G., Schär, C., Ruti, P.M., Castro, M. and Visconti, G. (1997) Validation of present-day

- regional climate simulations over Europe: LAM simulations with observed boundary conditions. *Climate Dynamics*, 13(7), 489–506.
- Collins, W.D., Rasch, P.J., Boville, B.A., Hack, J.J., McCaa, J.R., Williamson, D.L., Kiehl, J.T., Briegleb, B., Bitz, C., Lin, S.J., Zhang, M. and Dai, Y. (2004) Description of the NCAR community atmosphere model (CAM 3.0) *NCAR Technical Note*, 464+ STR
- Davies, H.C. (1976) A lateral boundary formulation for multi-level prediction models. *The Quarterly Journal of the Royal Meteorological Society*, 102(432), 405–418.
- Dee, D.P., Uppala, S.M., Simmons, A.J., Berrisford, P., Poli, P., Kobayashi, S., Andrae, U., Balmaseda, M.A., Balsamo, G., Bauer, P., Bechtold, P., Beljaars, A.C.M., van de Berg, L., Bidlot, J., Bormann, N., Delsol, C., Dragani, R., Fuentes, M., Geer, A.J., Haimberger, L., Healy, S.B., Hersbach, H., Hólm, E.V., Isaksen, L., Källberg, P., Köhler, M., Matricardi, M., McNally, A. P., Monge-Sanz, B.M., Morcrette, J.J., Park, B.K., Peubey, C., de Rosnay, P., Tavolato, C., Thépaut, J.N. and Vitart, F. (2011) The ERA-interim reanalysis: configuration and performance of the data assimilation system. *The Quarterly Journal of the Royal Meteorological Society*, 137(656), 553–597.
- Dickinson R.E., Henderson-Sellers A., Kennedy P.J. and Wilson M.F. (1993) Biosphere–atmosphere transfer scheme (BATS) version 1e as coupled to the NCAR Community Climate Model. *NCAR Technical Note*, 387+ STR.
- Doms, G. and Baldauf, M. (2015) *A description of the nonhydrostatic regional COSMO model part I: dynamics and numerics*. Offenbach, Germany: DWD.
- Dosio, A., Panitz, H.J., Schubert-Frisius, M. and Lüthi, D. (2015) Dynamical downscaling of cmip5 global circulation models over cordex-africa with cosmo-clm: evaluation over the present climate and analysis of the added value. *Climate Dynamics*, 44(9–10), 2637–2661.
- Emanuel, K.A. and Živković-Rothman, M. (1999) Development and Evaluation of a Convection Scheme for Use in Climate Models. *Journal of the Atmospheric Sciences*, 56, 1766–1782. [https://doi.org/10.1175/1520-0469\(1999\)056<1766:DAEOAC>2.0.CO;2](https://doi.org/10.1175/1520-0469(1999)056<1766:DAEOAC>2.0.CO;2).
- Fu, C., Wang, S., Xiong, Z., Gutowski, W.J., Lee, D.K., McGregor, J. L., Sato, Y., Kato, H., Kim, J.W. and Suh, M.S. (2005) Regional climate model intercomparison project (RMIP) for Asia. *The Bulletin of the American Meteorological Society*, 86(2), 257–266.
- Gao, X. and Giorgi, F. (2017) Use of the RegCM system over East Asia: review and perspectives. *Engineering*, 3(5), 766–772.
- Gao, X., Shi, Y., Song, R., Giorgi, F., Wang, Y. and Zhang, D. (2008) Reduction of future monsoon precipitation over China: comparison between a high resolution RCM simulation and the driving GCM. *Meteorology and Atmospheric Physics*, 100(1–4), 73–86.
- Giorgi, F., Francisco, R. and Pal, J. (2003) Effects of a subgrid-scale topography and land use scheme on the simulation of surface climate and hydrology. part i: effects of temperature and water vapor disaggregation. *Journal of Hydrometeorology*, 4(2), 317–333.
- Giorgi, F., Coppola, E., Solmon, F., Mariotti, L., Sylla, M.B., Bi, X., Elguindi, N., Diro, G.T., Nair, V., Giuliani, G., Turuncoglu, U.U., Cozzini, S., Gütterl, I., O'Brien, T.A., Tawfik, A.B., Shalaby, A., Zakey, A.S., Steiner, A.L., Stordal, F., Sloan, S.C. and Brankovic, C. (2012) RegCM4: model description and preliminary tests over multiple CORDEX domains. *Climate Research*, 52(1), 577X.
- Giorgi, F., Jones, C. and Asrar, G.R. (2009) Addressing climate information needs at the regional level: the CORDEX framework. *Bulletin -WMO*, 3, 175–183.
- Grell, G.A., Dudhia, J. and Stauffer, D.R. (1994) A Description of the Fifth-Generation Penn State/NCAR Mesoscale Model (MM5). *NCAR Technical Note*, 398+STR.
- Harris, I., Jones, P.D., Osborn, T.J. and Lister, D.H. (2014) Updated high-resolution grids of monthly climatic observations—the CRU TS3.10 dataset. *International Journal of Climatology*, 34(3), 623–642.
- Holtslag, A.A., DeBruijn, E.I. and Pan, H. (1990) A High Resolution Air Mass Transformation Model for Short-Range Weather Forecasting. *Monthly Weather Review*, 118, 1561–1575. [https://doi.org/10.1175/1520-0493\(1990\)118<1561:AHRAMT>2.0.CO;2](https://doi.org/10.1175/1520-0493(1990)118<1561:AHRAMT>2.0.CO;2).
- Hong, S., Dudhia, J. and Chen, S. (2004) A Revised Approach to Ice Microphysical Processes for the Bulk Parameterization of Cloudsand Precipitation. *Monthly Weather Review*, 132, 103–120. [https://doi.org/10.1175/1520-0493\(2004\)132<0103:ARATIM>2.0.CO;2](https://doi.org/10.1175/1520-0493(2004)132<0103:ARATIM>2.0.CO;2).
- Hong, S., Noh, Y. and Dudhia, J. (2006) A NewVertical Diffusion Package with an Explicit Treatment of Entrainment Processes. *Monthly Weather Review*, 134, 2318–2341. <https://doi.org/10.1175/MWR3199.1>.
- Hong, S.Y., Moon, N.K., Lim, K.S.S. and Kim, J.W. (2010) Future climate change scenarios over Korea using a multi-nested downscaling system: a pilot study. *Asia-Pacific Journal of Atmospheric Sciences*, 46(4), 425–435.
- Ji, Z. and Kang, S. (2015) Evaluation of extreme climate events using a regional climate model for China. *International Journal of Climatology*, 35(6), 888–902.
- Jiang, D. and Wang, H. (2005) Natural interdecadal weakening of East Asian summer monsoon in the late 20th century. *Chinese Science Bulletin*, 50(17), 1923–1929.
- Jin, C.S., Cha, D.H., Lee, D.K., Suh, M.S., Hong, S.Y., Kang, H.S. and Ho, C.H. (2016) Evaluation of climatological tropical cyclone activity over the western North Pacific in the CORDEX-East Asia multi-RCM simulations. *Climate Dynamics*, 47(3–4), 765–778.
- Kain, J.S. (2004) The Kain–Fritsch Convective Parameterization: An Update. *Journal of Applied Meteorology*, 43, 170–181.
- Kiehl, J.T., Hack, J.J., Bonan, G.B., Boville, B.A., Williamson, D.L. and Rasch, P.J. (1998) The National Center for Atmospheric Research Community Climate Model: CCM3. *Journal of Climate*, 11, 1131–1149.
- Kim, J., Waliser, D.E., Mattmann, C.A., Goodale, C.E., Hart, A.F., Zimdars, P.A., Crichton, D.J., Jones, C., Nikulin, G., Hewitson, B., Jack, C., Lennard, C. and Favre, A. (2014) Evaluation of the CORDEX-Africa multi-RCM hindcast: systematic model errors. *Climate Dynamics*, 42(5–6), 1189–1202.
- Kotlarski, S., Keuler, K., Christensen, O.B., Colette, A., Déqué, M., Gobiet, A., Goergen, K., Jacob, D., Lüthi, D., van Meijgaard, E., Nikulin, G., Schär, C., Teichmann, C., Vautard, R., Warrach-Sagi, K. and Wulfmeyer, V. (2014) Regional climate modelling on European scales: a joint standard evaluation of the EURO-CORDEX RCM ensemble. *Geoscientific Model Development Discussion*, 7(4), 1297–1333.
- Lau, N. and Poshay, J. (2009) Simulation of synoptic and sub-synoptic scale phenomena associated with the east asian monsoon using a high-resolution GCM. *Monthly Weather Review*, 137(1), 137–160.

- Lott, F. and Miller, M.J. (1997) A new subgrid-scale orographic drag parametrization: Its formulation and testing. *Quarterly Journal of the Royal Meteorological Society*, 123, 101–127. <https://doi.org/10.1002/qj.49712353704>.
- Mironov, D. and Raschendorfer, M. (2001) Evaluation of empirical parameters of the new LM surface-layer parameterization Scheme: results from numerical experiments including soil moisture analysis. COSMO technical report No.1. DWD, Offenbach, Germany, 12pp.
- Mukai, M., Nakajima, T. and Takemura, T. (2008) A study of anthropogenic impacts of the radiation budget and the cloud field in East Asia based on model simulations with GCM. *Journal of Geophysical Research*, 113(D12211).
- Ozturk, T., Altinsoy, H., Turke, M. and Kurnaz, M. (2012) Simulation of temperature and precipitation climatology for the Central Asia CORDEX domain using RegCM 4.0. *Climate Research*, 52(1), 63–76.
- Pal, J.S., Small, E.E. and Eltahir, E.A.B. (2000) Simulation of regional-scale water and energy budgets: Representation of subgrid cloud and precipitation processes within RegCM. *Journal of Geophysical Research: Atmospheres*, 105(D24), 29579–29594. <https://doi.org/10.1029/2000JD900415>.
- Park, C., Min, S.K., Lee, D., Cha, D.H., Suh, M.S., Kang, H.S., Hong, S.Y., Lee, D.K., Baek, H.J., Boo, K.O. and Kwon, W.T. (2016) Evaluation of multiple regional climate models for summer climate extremes over East Asia. *Climate Dynamics*, 46(7), 1–18.
- Park, J.H., Oh, S.G. and Suh, M.S. (2013) Impacts of boundary conditions on the precipitation simulation of RegCM4 in the CORDEX East Asia domain. *Journal of Geophysical Research*, 118(4), 1652–1667.
- Reynolds, R.W., Rayner, N.A., Smith, T.M., Stokes, D.C. and Wang, W. (2002) An improved in situ and satellite SST analysis for climate. *Journal of Climate*, 15, 1609–1625.
- Ritter, B. and Geleyn, J.F. (1992) A comprehensive radiation scheme for numerical weather prediction models with potential applications in climate simulations. *Monthly Weather Review*, 120, 303–325.
- Rockel, B., Will, A. and Hense, A. (2008) The regional climate model COSMO-CLM (CCLM). *Meteorologische Zeitschrift*, 17(4), 347–348.
- Rummukainen, M. (2010) State-of-the-art with regional climate models. *WIREs Climate Change*, 1(1), 82–96.
- Schrodin, R. and Heise, E. (2001) The Multi-Layer Version of the DWD Soil Model TERRA-LM. In: *COSMO Technical Report No. 2*. DWD, Offenbach, Germany, p. 16.
- Seifert, A. and Beheng, K.D. (2001) A double-moment parameterization for simulating auto conversion, accretion and selfcollection. *Atmospheric Research*, 59–60, 265–281.
- Shen, W., Tang, J., Wang, Y., Wang, S. and Niu, X. (2017) Evaluation of WRF model simulations of tropical cyclones in the western North Pacific over the CORDEX East Asia domain. *Climate Dynamics*, 48(7–8), 2419–2435.
- Shi, Y., Wang, G. and Gao, X. (2017) Role of resolution in regional climate change projections over China. *Climate Dynamics*, 51, 2375–2396.
- Skamarock, W.C., Klemp, J.B., Dudhia, J., Gill, D.O., Barker, D.M., Duda, M.G., Huang, X., Wang, W. and Powers, J.G. (2008) A description of the Advanced Research WRF version 3. *NCAR Technical Note 475+ STR*, 125.
- Song, F. and Zhou, T. (2014) Interannual variability of east Asian summer monsoon simulated by CMIP3 and CMIP5 AGCMs: skill dependence on Indian Ocean–Western Pacific anticyclone teleconnection. *Journal of Climate*, 27(4), 1679–1697.
- Sun, X., Xue, M., Brotzge, J., McPherson, R.A., Hu, X. and Yang, X. (2016) An evaluation of dynamical downscaling of Central Plains summer precipitation using a WRF-based regional climate model at a convection-permitting 4km resolution. *Journal of Geophysical Research*, 121(23), 13801–13825.
- Tang, J., Wang, S., Niu, X., Hui, P., Zong, P. and Wang, X. (2017) Impact of spectral nudging on regional climate simulation over CORDEX East Asia using WRF. *Climate Dynamics*, 48(7–8), 2339–2357.
- Tiedtke, M. (1989) A comprehensive massflux scheme for cumulus parameterization in large-scale models. *Monthly Weather Review*, 117, 1779–1800.
- Tselioudis, G., Douvis, C. and Zerefos, C. (2012) Does dynamical downscaling introduce novel information in climate model simulations of precipitation change over a complex topography region? *International Journal of Climatology*, 32(10), 1572–1578.
- Taylor, K.E. (2001) Summarizing multiple aspects of model performance in a single diagram. *Journal of Geophysical Research: Atmospheres*, 106, 7183–7192.
- Wang, P., Tang, J., Sun, X., Liu, J. and Fang, J. (2018) Spatiotemporal characteristics of heat waves over China in regional climate simulations within the CORDEX-EA project. *Climate Dynamics*, 52(1–2), 799–818.
- Wu, J. and Gao, X. (2013) A gridded daily observation dataset over China region and comparison with the other datasets. *The Chinese Journal of Geophysics (in Chinese)*, 56(4), 1102–1111.
- Yang, B., Zhou, Y., Zhang, Y., Huang, A., Qian, Y. and Zhang, L. (2017) Simulated precipitation diurnal cycles over East Asia using different CAPE-based convective closure schemes in WRF model. *Climate Dynamics*, 50(5–6), 1639–1658.
- Yao, S. and Zhang, Y. (2010) Simulation of China summer precipitation using a regional air-sea coupled model. *Acta Meteorologica Sinica*, 24(2), 203–214.
- Yhang, Y.B. and Hong, S.Y. (2006) Improved physical processes in a regional climate model and their impact on the simulated summer monsoon circulations over East Asia. *Journal of Climate*, 21(5), 963–979.
- Yu, E., Sun, J., Chen, H. and Xiang, W. (2015) Evaluation of a high-resolution historical simulation over China: climatology and extremes. *Climate Dynamics*, 45(7–8), 2013–2031.
- Zhao, D. (2013) Performance of regional integrated environment modelling system (RIEMS) in precipitation simulations over East Asia. *Climate Dynamics*, 40(7–8), 1767–1787.
- Zhou, T. and Zou, L. (2002) Simulation of the east asian summer monsoon using a variable resolution atmospheric GCM. *Climate Dynamics*, 19(2), 167–180.
- Zhou, W., Tang, J., Wang, X., Wang, S., Niu, X. and Wang, Y. (2016) Evaluation of regional climate simulations over the CORDEX-EA-II domain using the COSMO-CLM model. *Asia-Pacific Journal of Atmospheric Sciences*, 52(2), 107–127.
- Zou, L., Qian, Y., Zhou, T. and Yang, B. (2014) Parameter tuning and calibration of RegCM3 with MIT–Emanuel cumulus parameterization scheme over CORDEX East Asia domain. *Journal of Climate*, 27(20), 7687–7701.

- Zou, L. and Zhou, T. (2013) Can a regional ocean-atmosphere coupled model improve the simulation of the interannual variability of the Western North Pacific summer monsoon? *Journal of Climate*, 26 (7), 2353–2367.
- Zou, L. and Zhou, T. (2016) Future summer precipitation changes over CORDEX-East Asia domain downscaled by a regional ocean-atmosphere coupled model: a comparison to the stand-alone RCM. *Journal of Geophysical Research*, 121(6), 2691–2704.
- Zou, L., Zhou, T. and Peng, D. (2016) Dynamical downscaling of historical climate over CORDEX East Asia domain: a comparison of regional ocean-atmosphere coupled model to stand-alone RCM simulations. *Journal of Geophysical Research*, 121(4), 1442–1458.

SUPPORTING INFORMATION

Additional supporting information may be found online in the Supporting Information section at the end of this article.

How to cite this article: Yu K, Hui P, Zhou W, Tang J. Evaluation of multi-RCM high-resolution hindcast over the CORDEX East Asia Phase II region: Mean, annual cycle and interannual variations. *Int J Climatol*. 2019;1–19. <https://doi.org/10.1002/joc.6323>